Full-Scale Tests of Butt-Welded Splices in Heavy-Rolled Steel Sections Subjected to Primary Tensile Stresses

MICHEL BRUNEAU and STEPHEN A. MAHIN

ABSTRACT

Experimental results from full-scale testing of full and partial penetration butt-welded capacity. Qualitative explanations are given as to the cause of the observed failure. The splice with full penetration welds exhibited satisfactory strength and ductility. It is believed that a great amount of care must be taken in the execution of this weld type. Future research needs are examined.

INTRODUCTION

Structural steel sections in Groups 4 and 5 are extensively used as compression members in tall buildings and other large structures. In a number of instances, welded butt splices in tension members fabricated from Group 4 and 5 sections would appear to provide a good solution to common design problems. However, the AISC[2] currently does not recommend the use of such sections in designs requiring welding or thermal cutting unless the adequacy of material properties for such applications are determined. Furthermore, an AISC Supplement, effective since January 1989, as well as the 1989 ASD Specification, requires Charpy V-notch test results to be specified if full penetration welds are to be performed.

Several cases of partial or complete brittle fracture have been reported during fabrication or construction when welded splices of jumbo sections were subjected to tension.[4,10,13,20] A wide variety of opinions have been expressed as to the cause for this unsatisfactory performance. Some have attributed these problems to the microstructural features and segregation (especially in the region contiguous to the flange and web) that occur in such sections due to relatively high alloying, limited rolling and high finish temperatures employed in their manufacture. Others allege that the unsatisfactory performance is a result of inadequate weld design or the use of improper or poorly executed welding procedures. This situation casts considerable uncertainty as to the safety and use of these types of members in tension.

Michel Bruneau is assistant professor, Civil Engineering Department, University of Ottawa, Ottawa, Ontario, Canada.

Stephen A. Mahin is professor, Department of Civil Engineering, University of California, Berkeley, CA.

Unfortunately, there is relatively little quantitative information available in the literature related to the experimental behavior of field performance of tension splices in heavy section members. Welds in thick steel plates have been known for years to be problem-prone in general. With the increase in steel thickness and amount of weld material deposited, problems such as lamellar tearing, weld embrittlement, underbead cracking, distortion, and so on have been observed to occur more frequently. Several papers are available in the literature on the basic causes of these types of problems and general fabrication techniques to be used to minimize their occurrence. However, nearly all of this information is of qualitative nature.[1,5,6,10,16,22]

Detailed reports of the findings of structural failure investigations have been few. In one prominent reported case,[10] a full penetration butt weld (flanges and web fully welded) was located in the tension chord of a heavy truss. It failed brittly, resulting in the collapse of the truss during construction. The specific cause of the failure appears to be linked to high residual stresses and the particularly low notch toughness of the base material at the failed joint. The weld design and process used resulted in an initial crack, which, while stable under the self-weight of the truss, propagated brittly as the service loads increased during construction.

Little quantitative laboratory data have been published on the mechanical behavior of splices in jumbo sections. Much of the available data relates to welding procedure qualification tests (without data related to mechanical performance), to metallurgical design studies of special consumables, and to bend or impact acceptance-type tests of butt welds in thick plates or coupons. Some pure tension tests of tension splices in Group 4 and 5 sections have been reported[15] for specimens having only their flanges welded and for which, in some instances, significant portions of flanges were trimmed to accommodate experimental constraints. These sections were able to develop their calculated capacities, but in general most sections exhibited very little ductility. These experiments hint that ductility in large sections can be disappointing.

The aforementioned reported brittle failures of heavy welded steel sections have raised serious questions in California, where structural engineers often use jumbo section welded details in columns of earthquake-resistant structural steel systems. The ductility of such assemblages can be of major importance in these cases, and the scarcity of

available quantitative experimental data documenting the ultimate behavior of such full-scale welded splices pose a problem to designers in seismically active regions. In that perspective, a testing program was conducted to investigate the behavior of partial and full penetration butt-weld splices of typical Group 4 and 5 sections representative of California's column-splice splices of ASTM A6 Group 4 and 5 heavy-rolled sections are presented. Welded splices of the test specimens were subjected to primary tensile stresses as induced by pure bending. The partial penetration splice failed in a brittle manner with no apparent ductility. However, it was able to develop and exceed its nominal detailing practice.

After briefly reviewing the factors which are likely to affect the behavior of welded splices in heavy steel sections, the research program is described. The test results are presented and compared with analyses in order to assess the design implications and identify future research needs. Additional information on this testing program may be found in Ref. 7.

FACTORS ADVERSELY AFFECTING THE BEHAVIOR OF WELDED SPLICES IN HEAVY STEEL SECTIONS

Numerous factors tend to promote crack initiation and propagation in heavy steel sections. Those pertinent to the case at hand are briefly reviewed below. The concurrent presence of these factors with restraint-induced triaxial stress state may inhibit the ability of ductile steel to deform in a ductile manner.

1. The high carbon content of the A572 grade steel widely used in practice is propitious to crack initiation. The A.W.S. Handbook[3] specifies that for an equivalent carbon content (C.E.) above 40, there is a potential for cracking in the heat affected zones near flame cut edges and welds. A572 steel can have a C.E. in excess of 50 and therefore has a high cracking potential.

2. Extensive analysis of the metallurgy of heavy steel rolled sections by Fisher and Pense may have revealed a weakness in the fracture resistance (K_{IC}) of many of these sections, especially in the web-flange core area. This area of a jumbo section does not get worked during the rolling process to the degree that smaller sections do. It has a "cast-like" structure with large grains and inherently less fracture toughness.[10] Moving away from the web-flange intersection core, a progressively improving fracture toughness is obtained as one gets closer to the outer-surface of the flanges, the flange tips, or the bottom surface of flanges away from the web-flange core. This is in spite of adequate and constant yield stress properties throughout the flange. Values of fracture toughness K_{IC} and yield stress σ_y are not related properties of steel in general.

3. Flame-cut weld-access holes in webs near the flange will generally create an irregular surface along the cope, and also modify the metallurgy of the steel along a narrow strip adjacent to the cope, usually not more than a few sixteenths of an inch deep. This martensite transformation along the inevitable roughened surface promotes crack formation. The weld-access hole is not only often necessary to make a sound weld, but also desirable, as it effectively acts as a stress relief hole by reducing the transverse restraint on the flange welds. When these holes must be flame-cut, it has been recommended that the martensite region created be ground smooth prior to welding.[4,10]

The above factors create an environment favorable for crack initiation and propagation, but an active external factor is needed to trigger the fracture process. The residual stresses induced by restrained weld shrinkage can provide this necessary additional factor. The welding sequence and weld configuration can induce very severe restraints on the weld shrinkage during cooling. Using existing qualitative information on weld shrinkage and distortion,[3,6] a simple observation of the weld's shrinkage orientation can provide insight in the triaxial stress state at the end of a flame-cut cope. For the example presented in Fig. 1, the weld sequence is assumed to have been initiated with a root pass on each flange, followed by welding of the web, outside of the flanges, and finally the inside of the flanges.

Due to the presence of the root weld between the flanges, the web welds would induce tension in the vertical plane (noted **1*** on the triaxial stress diagram in Fig. 1), but the weld-access hole, when present, can effectively reduce this component of residual stresses.

More critical is the welding of the outside of the flanges prior to the inside of the flanges. As shown in Fig. 2, this creates a tendency of the flanges to rotate (bow) away from the web. Therefore, the web-flange region at the end of the cope (which has been reported to have a lower fracture resistance) is stressed in tension and an initial crack could propagate further. Crack propagation reduces the flange curvature which in turn results in a lower tensile force at the end of the cope, and the failure process could conceivably stop once the initial crack reaches a finite length. The final path followed by the crack will depend on the magnitude of all the components of the triaxial stress state shown on Fig. 1. This initial crack may rest in a stable position until external loads applied to the structure raise the stresses to the threshold where crack propagation will resume up to the total fracture of the section. Final cracking through the flange can be treated using fracture mechanics of a medium with a crack discontinuity.

From the above, it should be obvious that welding of the inside of the flanges prior to the outside of the flanges might have exactly the opposite effect. In that reversed sequence, the low fracture resistance web-flange region would be stressed in compression, as the welding of the inside of the flanges would be executed first; this reversed sequence for flange welding might not initiate critical cracks. Thus,

assuming invariant material properties, it is preferable to choose a weld design and process to minimize the occurrence and propagation of those initial cracks, but it is noteworthy that benefits ensuing from an optimal welding sequence can be negated by the execution of weld repairs.

RESEARCH PROGRAM

Background

A series of experimental and analytical studies were undertaken to provide quantitative data regarding the mechanical behavior of splices in Group 4 and 5 sections. Welded splice configurations considered were taken, at the recommendation of an Advisory Panel, to be representative of those used in columns of buildings located in seismically active regions; there was no intent to replicate splice details

used in actual reported failures. Still, full penetration weldments were the initial focus of these investigations because of the recorded history of field difficulties and performance failures of this class of splices in general. However, the Advisory Panel suggested that partial penetration splices also be investigated, as they represent the substantial majority of all the welds used for column splices. Special attention was placed on making the specimens representative of current engineering and fabrication practices. Consequently, in these investigations, no efforts were made to modify the metallurgical properties of the base metal or to develop special purpose weld procedures.

Engineers will often specify a partial penetration weld of 50% of the flanges (T/2) and 50% of the web (W/2) (Fig. 3) for use in seismic regions. This configuration also corresponds to a minimum weld detail for some codes in
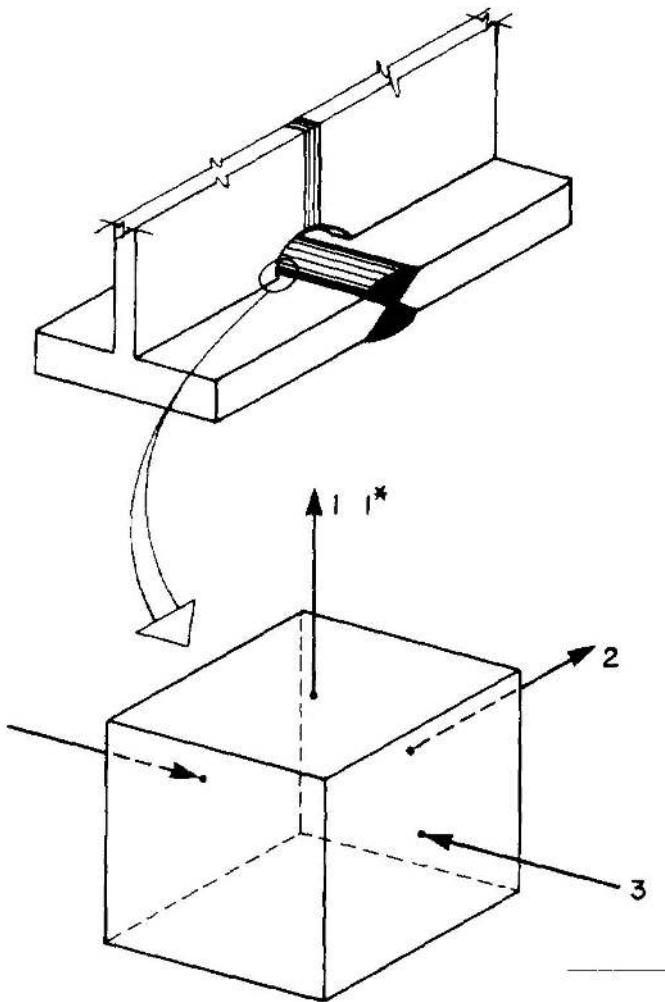

1. Tension due to tendency of flange to distort
1.* Tension due to high restraint against longitudinal shrinkoge of web welds (may not be present if cope holes large enough)
2. Tension: Tronsverse welding restraint of flange
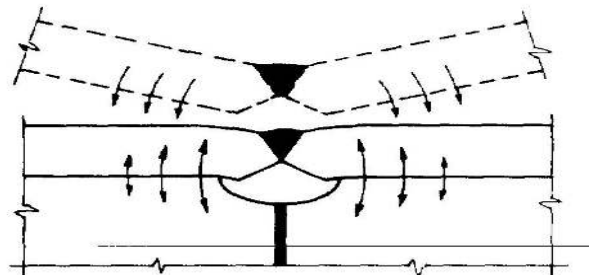3. Compression due to longitudinal shrinkage of flange welds

Fig. 1.   *Qualitative illustration of the triaxial state of stress at the point of cracking initiation.*
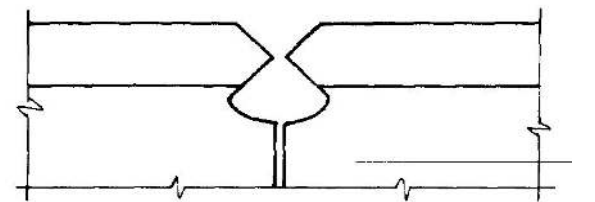
A.   BEFORE WELDING THE FLANGES
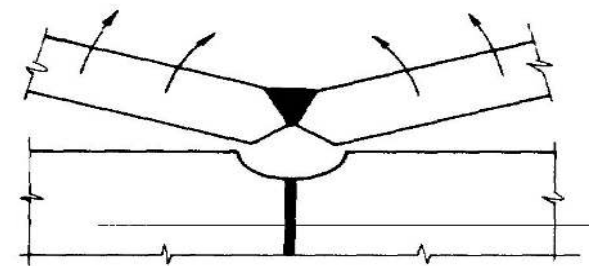
B.   WELDING OF THE OUTSIDE OF
     FLANGES CAUSE TENDENCY TO LIFT

C.   BY PULLING ACTION OF THE WEB,
     THE FLANGE STAYS IN PLACE
     BUT TENSION RESIDUAL STRESSES
     ARE INDUCED

Fig. 2.   *Qualitative illustration of the effect of weld shrinkage on internal stresses.*

specific circumstances. For example, the Uniform Building Code[21] requires this for trusses (Sect. 2712g), and the SEAOC "Recommended Lateral Force Requirements and Commentary"[19] stipulates it for columns when there is any net calculable tensile force (1988, Sect. 4-d). When full penetration welds are specified for building columns, they are often detailed with the flanges completely welded (T) and the web partially welded (W/2) (Fig. 4). Therefore, a partial penetration connection and a full penetration one as described above were selected for testing.

Test Specimen Configuration

It was originally intended that pure tension tests would be performed on the splice specimens, since field problems had been reported under such a loading condition. However, preliminary designs of specimens utilizing the very large sections of interest indicated that a big portion of the ends of the flanges would have to be trimmed to accommodate the 4 million pound limit of the available test machine. Cutting away part of the section would have released some of the locked-in residual stresses that might have contributed to the observed failures. Moreover, removal of the material from the tips of the flanges (where better microstructural features exist) might adversely affect performance.

Therefore, in order to test sections as big as possible and to make the specimens representative of column behavior under seismic loading conditions, it was decided to test specimens in bending. Several possibilities for considering axial load and shear effects were evaluated. Since the

absence of axial load provided a conservative condition and simplified subsequent interpretation of data, it was decided to ignore axial load effects in these tests. While it was possible to apply shear to the splice, it was not possible to obtain a consensus on what a realistic value of shear force might be. Thus, for these tests, it was decided to test the splice under pure moment.
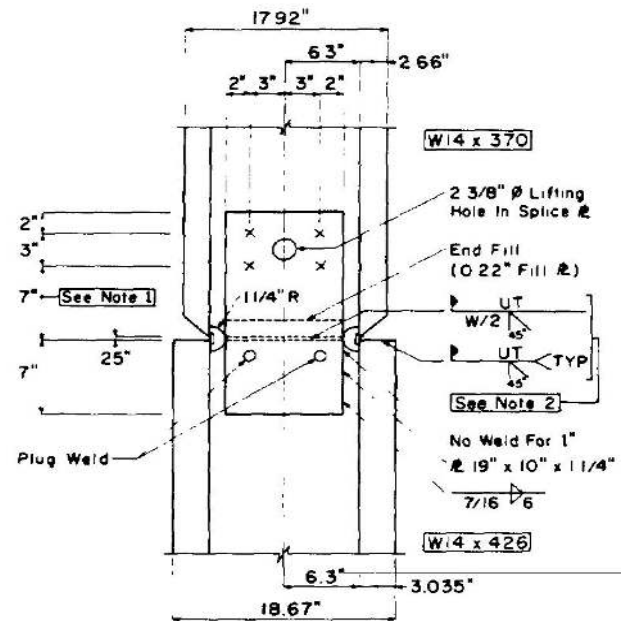
A typical test setup is illustrated in Fig. 5. The load applied by the testing machine head is split, through a spreader beam, into two point loads (rollers) acting on the specimen to create the uniform moment region. The size of that region was selected considering the St. Venant effect and the need to develop a regular stress distribution in front of the splice. The minimum required length of the specimen
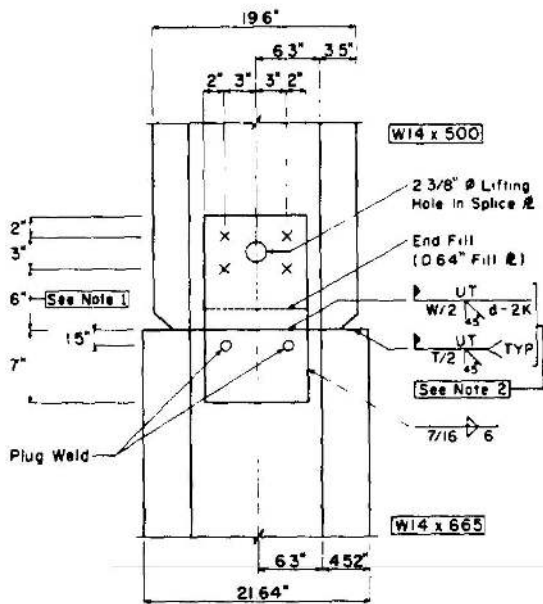
Fig. 4.   Test specimen for full penetration welded splice detail.
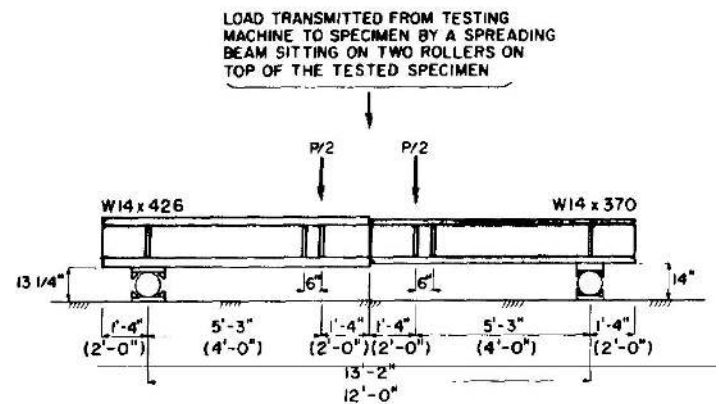

Fig. 5.   Specimen setup for full penetration test (partial penetration test specimen dimensions in parentheses).

Fig. 3.   Test specimen for partial penetration welded splice detail.

from the load point to the support was dictated by the maximum shear that could be carried by a specimen's web, as the load necessary to yield the splice in bending must be less than that needed to yield the web in shear. The maximum total length of the specimen is, in turn, limited by the physical size of the testing machine table. These restrictions, taken together, imposed the only limits on the size of specimen that could be accommodated. It proved to be a limiting factor only for the full penetration test, where the largest specimen could not exceed approximately 400 lbs/ft.

Specimens for these experiments were fabricated from standard A572 Grade 50 steel. It should be noted that A572 Grade 50 steel has been involved in all the reported splice failures.[4,10,20] All steel grades may not develop similar adverse behavior. However, A572 Grade 50 steel is believed to be more widely used. It also has a lower notch toughness than A36 Grade steel, which makes it more susceptible, from a fracture mechanics point of view.

In all cases, the tested connection was to represent a building column splice as executed in the field. The specimens were executed using standard fabricator details and procedures for field splices. Details of the weld design (cope dimensions, bevel design, etc.) were proposed by the fabricators, who were asked to submit their details for review prior to fabrication. Splice welds were executed in the shop with the specimens in an upright position, simulating, as much as possible, field conditions and procedures. Furthermore, inspectors witnessed the operations, verified that AWS preheat, interpass and post-heat requirements were respected, and performed ultrasonic testing of the base metal and of the welds to insure conformity to AWS standards. The weld process was FCAW using E70 electrodes.

Sample Weld

A short stub column was welded and cut in order to allow visual observation of the weld. The weld surfaces were polished and etched. The dendritic crystalline formation is clearly visible on the full penetration flange weld of Fig. 6. The flange shown is 3.5 in. thick. It is very interesting to see the crack-like effect at the toe of a typical partial penetration weld. Figure 7 shows a half penetration weld of a 3.5 in. thick flange. Some of the welds contained small voids that could act like stress raisers.

Specimen 1—Partial Penetration Weld. A W14×500 was connected to a W14×665 by a partial penetration butt weld. These are among the biggest rolled sections available from the AISC handbook. The splice area was preheated to 250°F and the interpass temperature was controlled during execution of the weld. The welding sequence adopted by the fabricator for this partial penetration butt weld is as follows: Three passes on the web, three passes on one flange, three on the other flange, completion of the web weld, and final welding of the flanges by alternatively performing approximately six passes at a time on each flange, until there

is a smooth transition from the thicker flange to the thinner flange at the connection. The fabricator judged the ambient temperature of about 70°F to be sufficiently warm so that the specimen could be air cooled. Visual inspection and ultrasonic inspection of the base metal and weld were executed, and no defects were reported.

Specimen 2—Full Penetration Weld. A W14×370 was connected to a W14×426 by a full penetration butt weld. These were practically the largest section sizes that could be accommodated on the testing machine with a full penetration splice. The web of the outer portion of the W14×370 was expected to approach its shear yielding capacity V_p when the splice region would reach its flexural moment capacity M_p. Therefore, additional stiffeners were added to help the transfer of shear in this critical region, thus protecting the section against an undesirable local failure mode.

The weld-access holes at the web-flange intersection were ground smooth as was the custom with the fabricator. This provided a smooth surface in the critical zone of the metal where the metallurgy is of inferior quality. In previously reported failure case studies,[10] flame-cut copes cr-

Fig. 6. Dendritic crystalline formation on a polished and etched full penetration weld on a thick flange.

eated avery jagged and brittle martensite surface that served as crack initiators. The grinding of these flame-cut copes should be noted when interpreting the test results. Another special feature to be noted was that the root pass for the flange welds was located in the backup bars.

The specimen was preheated to 250°F. The web weld was executed completely before welding the flanges. The flanges were welded in an alternative manner with approximately six passes at a time on each flange. Interpass temperature was controlled. E70 low hydrogen electrodes were used. After completion of the weld, the splice area was wrapped with a thermal blanket to help slow cooling overnight. Ambient temperatures at the time of welding were estimated to be between 60 and 70°F. Ultrasonic inspection of the base metal and weld were executed, and no defects were reported.

TEST RESULTS FOR SPECIMEN NO. 1

Description of Testing

The weakest link in the specimen is obviously the partial penetration weld, as it is expected to be able to transfer only about half of the capacity of the smaller section connected.
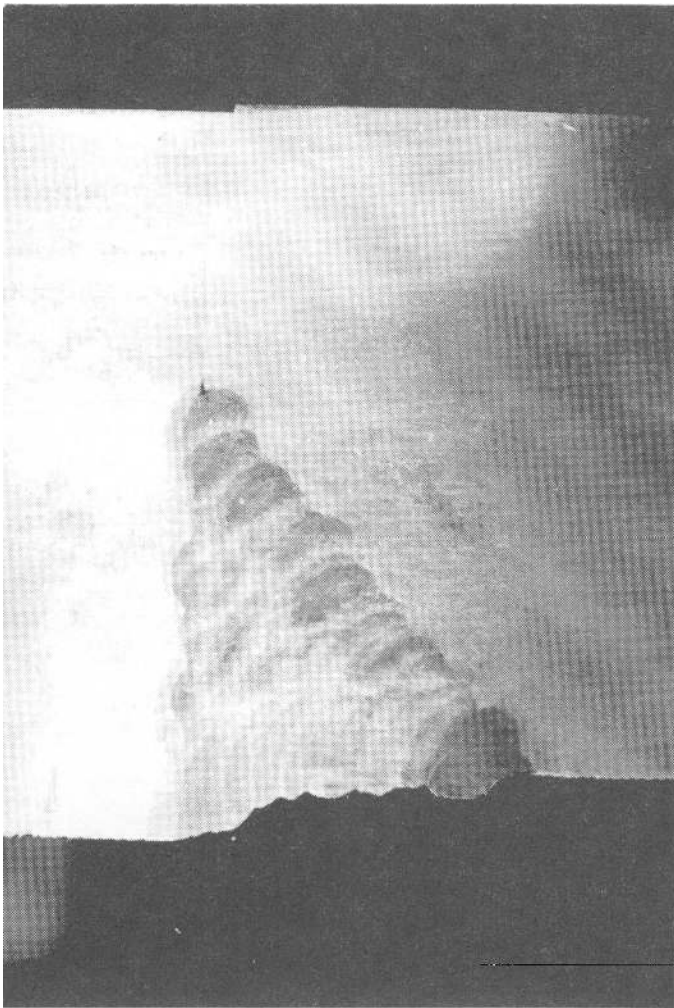

Fig. 7. Polished and etched half penetration weld on a thick flange.

The yield stress of steel is presumably lower than that of the matching weld material, and consequently any yielding of Specimen 1 was expected to be concentrated in the steel immediately adjacent to the weld area.

Consequently, an X-Y plot of the moment-curvature relationship (as measured by clip gages on a 6¾-in. gage length) at the center splice was used to monitor the behavior of the splice as the loading program progressed. A total of 29 channels of data were recorded for subsequent evaluation (Fig. 8). These included pairs of clip gages to allow curvatures to be computed at various points near the splice. Linear Variable Differential Transducers (LVDTs) were also installed to measure the opening of the inside (unpenetrated) face of the tension flange. Two LVDTs were used to measure the midspan deflection of the beam. Strain gages were installed on the web to help identify the movement of the neutral axis and to provide another indicator of curvature near the splice. The load applied to the beam was also monitored. All data was recorded by a microcomputer-based data acquisition system.

The initial phase of the testing was to gradually load the specimen to its nominal capacity and continue until it evidenced a small plastic offset in the moment-curvature curve (say 0.5% as used to measure initial yield stress in materials). The specimen would then be inverted for subsequent loading. In this first step of the testing program, loading was applied at a rate of about 3.2 kips/sec. Loading exceeded theoretical values of $M_y/2$ and $M_p/2$ for the smaller section (assuming nominal yield value of 50 ksi) without difficulty. This latter value corresponded to an applied load of 1100 kips. Since the moment-curvature plot revealed no signs of non-linearity, the loading was incremented to 1200 kips, which corresponds to the theoretical full-yield state of a fictitious steel cross-section created by the welded surfaces (i.e., half the flanges and half the web of the smaller section). This was thought to be another way a designer would likely estimate the capacity of the splice. Thus, the theoretical capacity of the section based on specified yield stress was attained without apparent signs of significant yielding distress in the specimen.
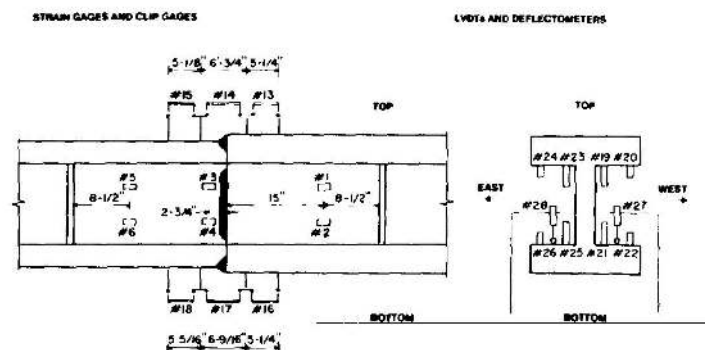

Fig. 8. Location of recording instruments on partial penetration splice specimen.

There was a 30-second pause at that point (which produced a negligible 13 kips loss of load) to make sure non-linearity of the splice had not started to occur. Visual inspection of the plotted splice moment-curvature record and of the other printed transducer measurements still showed no sign of significant yielding. It was consequently decided to continue the loading. The subsequent rate of loading was reduced to 1.6 kip/sec. The moment-curvature relationship was observed to remain practically linear up to approximately 1475 kips (the last digitized value was 1458 kips) when a sudden and brittle failure occurred through the weld. Failure was complete (Fig. 9) and very loud.

Once failure started in the tension (bottom) flange, the remaining unfailed part of the section was unable to accommodate the imposed displacement. The failure then quickly progressed through the whole section. The erection plate (Fig. 9) did not help restrain or stabilize the failure once it initiated. The erection bolts sheared suddenly and they were thrown with considerable energy away from the splice.

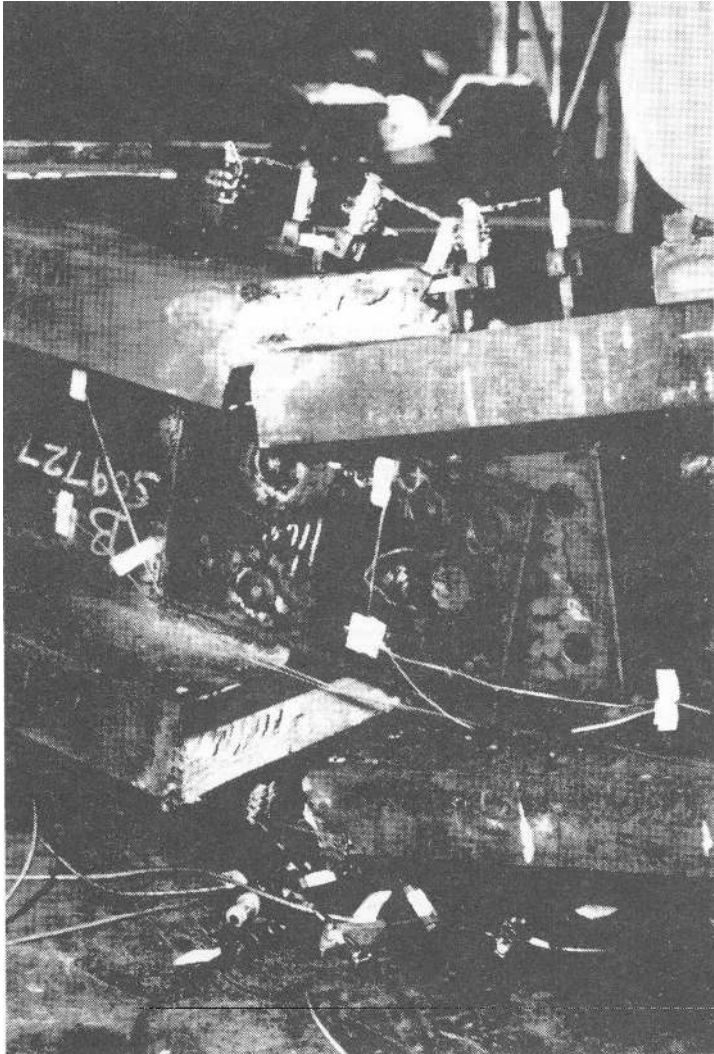Temperature at time of testing was around 55°F (13°C).

Analysis of Failure Surface

Since failure occurred through the weld (Fig. 10), the failure surface was carefully investigated. The failure surface was nearly planar and followed the juncture of the two sections. At this location the weld was thickest, extending from the mid-depth of the thinner flange to the top of the thicker flange. After inspecting the failure surface, a welding consultant[8] indicated the following:

- The welds were rated as poor welds because of lack of fusion between passes (individual passes were very pronounced and the passes in the surface of the welds had valleys between passes and most of the fracture surfaces were between passes), lack of penetration and fusion of root passes (as much as $\frac{1}{8}$ in. of the prepared 45° bevel being unfused in several places), and some other minor controversial metallurgical items (large columnar grain growth in some of the weld beads).
- The brittle mode of failure was virtually assured by the lateral restraint of the welds being welded to the
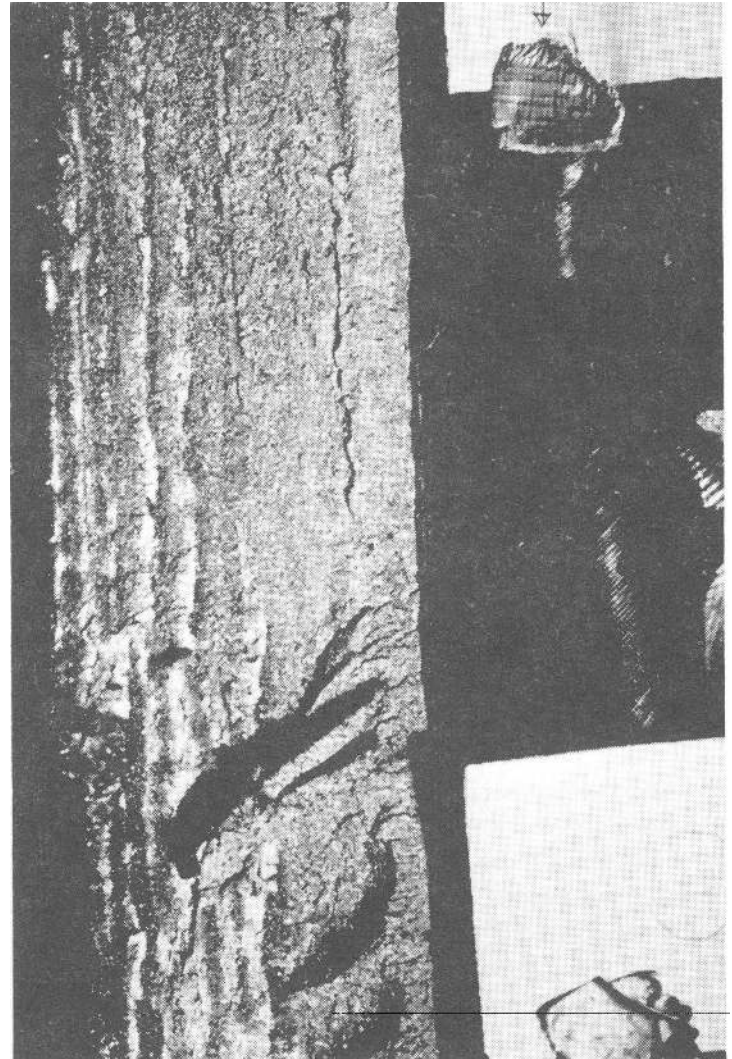

Fig. 9. Failure of partial penetration welded splice.

Fig. 10. Failure surface of partial penetration welded splice—center of bottom flange.

large jumbo sections, which restricted the reduction in area (necking down) of the welds; the "zero-gauge-length" effect, due to the very short length of the welds, which prevented the elongation of the welds in the longitudinal direction; the large stress concentration factors in the rupture section; and the placing of the splice welds in pure tension.

- Even with a very good weld, the splice weld would still fracture in a brittle mode, but the deposited weld metal, being stronger than the base metal, would tear out a nugget of the base metal, mainly because the reduction in area of the weld and the elongation of the weld are both restricted.

Fracture mechanics specimens (to evaluate K_{IC}) would usually have to be extracted, but since, in this case, the failure occurred through the weld, the value of this kind of test becomes uncertain. The K_{IC} value of steel is not relevant for this situation, and K_{IC} of the weld could not be obtained since the weld was destroyed. Furthermore, the applicability of stress intensity factors to large multipass welds is not well defined, since it is believed that a crack would simply propagate through the weakest link between the passes. Nevertheless, a value of K_I at failure can be roughly estimated, if the material is assumed continuous. It is accurate enough, in these circumstances, to use the equation for an elliptical thumbnail surface crack in a plate subjected to a uniform tensile stress where the major axis of the ellipse is infinity. The relevant equation is:[17]

$$K_I = 1.12\sigma(\pi a/Q)^{0.5}$$

where:

σ = applied stress
a = crack length (1.75 in. here)
Q = crack shape factor

The crack shape factor is a function of the ratio of the crack length over the thickness of the specimen, of the ratio of the major and minor axis of the elliptical crack (here a divided by infinity is taken to be zero), and of the ratio of the nominal applied stress to yield stress (this is intended to account for the effects of plastic deformation in the vicinity of the crack tip on the stress-intensity-factor value). Here, infinite thickness of the section is assumed in order to simulate the restraining effect of the web against bending deflection induced by the crack eccentricity.

Assuming the mean stress near the top of the flange far from the crack to be 29 ksi and that $Q = 0.85$,[18] the resulting stress-intensity factor would be $K_I = 83$ ksi $\sqrt{\text{in}}$ At a mean stress of 50 ksi, Q would reduce to 0.75, and K_I becomes 152 ksi $\sqrt{\text{in}}$ More conservative estimates would neglect the Q factor entirely, as there is no evidence that plastic deformations could be present in the vicinity of the crack tip as rupture progressed in the weld through a lack-of-fusion zone. Resulting values would be K_I of 76 and 131 ksi $\sqrt{\text{in}}$ for respective applied stresses of 29 and 50 ksi.

Analysis from Recorded Results

As expected, the load-deflection (P - δ) curve (Fig. 11) is not a good indicator of localizing yielding around the weld. The P - δ relationship is almost linear up to failure, but close inspection of the curve reveals a sudden change of stiffness at around 200 kips (the system becoming stiffer) and a very slight departure from a straight line at around 1200 kips (softening of the system). Table 1 compares the measured deflection with the ones calculated by linear elastic analyses under various assumptions. The best match of measured and calculated deflections is obtained when the proper respective moments of inertia are considered, the shear areas used are equal to the area of webs only (no participation from the flanges), and a short member (2 in. long) with a reduced moment of inertia equal to the splice stiffness (approximately $I/2$) is used to connect the two steel sections. Furthermore, in order to correct the effect of the initial "softness" of the setup, the experimental load-deflection curve has been shifted such that extrapolation of the elastic slope from 200 kips to 1200 kips defines a new origin at zero load. The computed deflections are still about 9% stiffer than the shifted experimental one, but it must be realized that the measured values include the deformation of the rollers, supports, and very likely some contribution from the testing machine (especially since the specimen was supported on the very corners of the base table).

The existence of an initially softer P - δ relationship is not entirely explained. A small gap could have been present between the two steel sections at the welds, and its closing on the compression flange side could have increased slightly the stiffness of the specimen. Also contributing to this may be the settling of the apparatus (rollers, plates, etc.), as the initial contact may not have been perfectly fit.

The strain gages, installed on the web of the specimen at three different locations (Fig. 8), produced additional useful information. Clusters of four gages (a pair on each side of the web) were placed on each section away from the splice and on the smaller section near the splice (where two of the
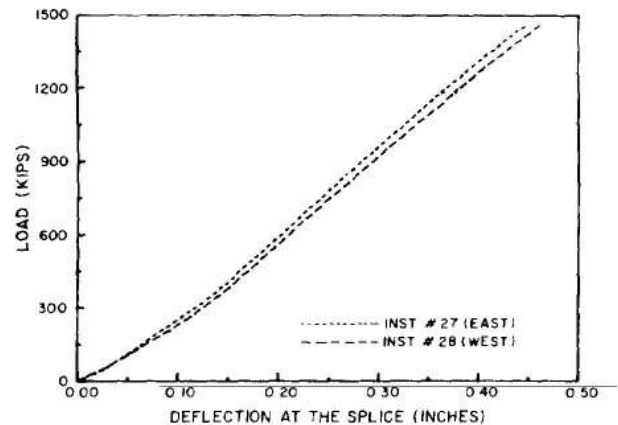

Fig. 11. Center span deflection for partial penetration specimen.

Load P (kips)	Measured (in.)	Shifted Measured[*]	Bending Rigid Splice	Only Flexible Splice	Bending Rigid Splice	Shear Flexible Splice[*]
102.3	.0481	–	.0183	.0189	.0251	.0257
202.2	.0863	–	.0362	.0373	.0496	.0509
302.5	.1218	.080	.0541	.0558	.0743	.0761
404.4	.1533	.1113	.0724	.0746	.0993	.1017
506.2	.1807	.1387	.0906	.0934	.1243	.1273
603.8	.2074	.1654	.1081	.1114	.1482	.1519
700.6	.2329	.1909	.1254	.1293	.1720	.1762
799.8	.2602	.2182	.1432	.1476	.1964	.2011
901.2	.2883	.2463	.1613	.1663	.2212	.2267
1002	.3169	.2749	.1794	.1849	.2460	.2520
1099	.3455	.3035	.1967	.2028	.2698	.2764
1194	.3717	.3297	.2137	.2203	.2931	.3003
1296	.4028	.3608	.2320	.2391	.3182	.3259
1399	.4351	.3931	.2504	.2581	.3435	.3518
1458	.4538	.4118	.2610	.2690	.3579	.3667

Table 1.
Comparison of Calculated vs. Measured Deflection

* Shifted measured deflection and bending + shear + flexible splice compare favorably (within 9% most of the time), the measured being larger than the predicted.

gages were placed on the erection plate). In the elastic range, moment-curvature relationships obtained from pairs of gages located on web (Fig. 12) are all equal to those predicted theoretically, within an acceptable accuracy. These relationships remained linear for most gaged sections except for the set on the W14×500's web near the splice which shows a slight softening near failure. This non-linearity recorded just before failure is an indicator of the initiation of yielding near the splice. The ratio of the maximum strain at this section to that further down the W14×500 (elastic) was only 1.05. This ratio can be an acceptable approximation of curvature ductility for small values of ductility. Nevertheless, the actual amount of yielding near the weld may have been larger than measured, as the gages were located 2¾ in. from the face of the splice.

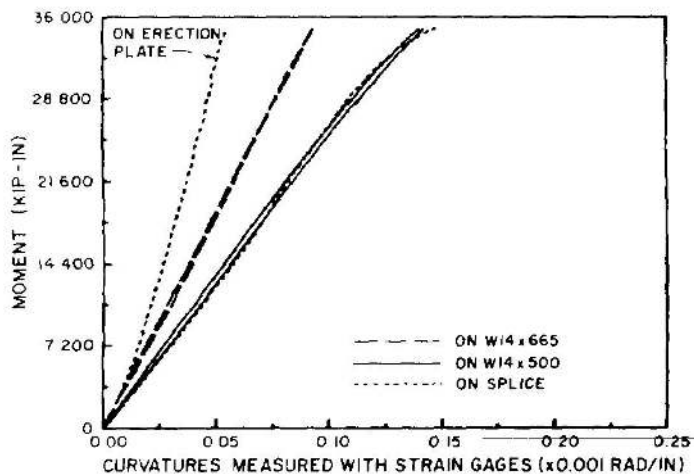Readings from the strain-gage set located on the erection

Fig. 12. Moment-curvature from strain gages on partial penetration specimen.

plate indicated that the plate contributed little to the actual resistance. The shear required from the bolts to produce the inferred maximum moment in the erection plate has been evaluated and was below the maximum allowable shear for this type of bolt. Therefore, failure did not originate at the bolts.

As shown in Fig. 8, LVDTs were located on the inside faces of the splice to measure opening (and closing) of the unpenetrated portion of the splice interface. LVDTs measured the change in distance between their connection points to the specimen; thus, measured displacements include not only the strains in the material but also crack opening in the tension region of the flange (or closing in the compression region, if an initial gap was present). Although LVDT readings were normalized by their gage length, and can only be qualitatively analyzed, they provide valuable information on the specimen's behavior and help substantiate the assertion that only very localized yielding occurred before failure. The LVDT readings are shown to be strongly non-linear on the tension flange and practically linear on the compression side (Figs. 13 and 14). This is an indication that there is a strong crack opening effect which is a non-linear function of the load increase.

The most meaningful information was provided by three pairs of clip gages with gage lengths of approximately 6 in. (Fig. 15). All measured moment-curvature relationships in the elastic range are almost perfectly equal to their theoretically calculated ones, with the W14×665 shown to remain perfectly elastic until failure of the specimen. Also, as the loads get above the 1200 kips level (equivalent to the 28,800 kip-in. moment level), a slight softening of the moment-curvature relation can be observed on the W14×500

near the splice, which is a good indication of local yielding. At failure, the curvatures did not exceed the predicted elastic values by more than 10%.
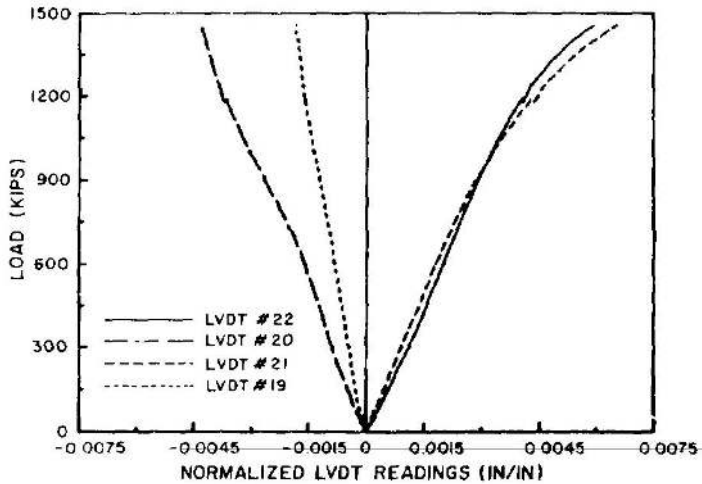

Fig. 13. Normalized readings for west-side LVDTs on partial penetration specimen.
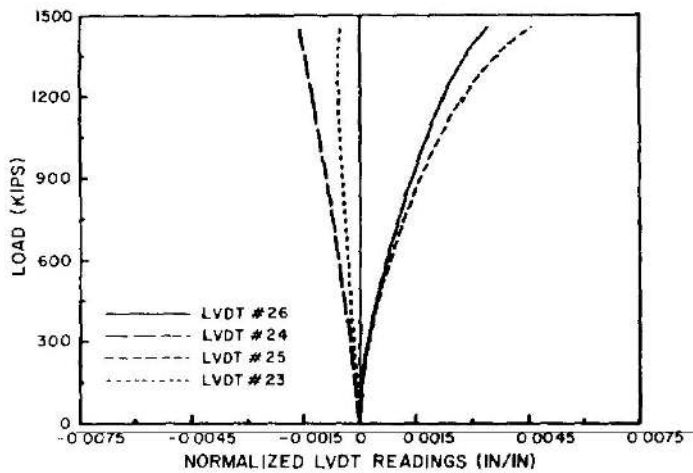

Fig. 14. Normalized readings for east-side LVDTs on partial penetration specimen.
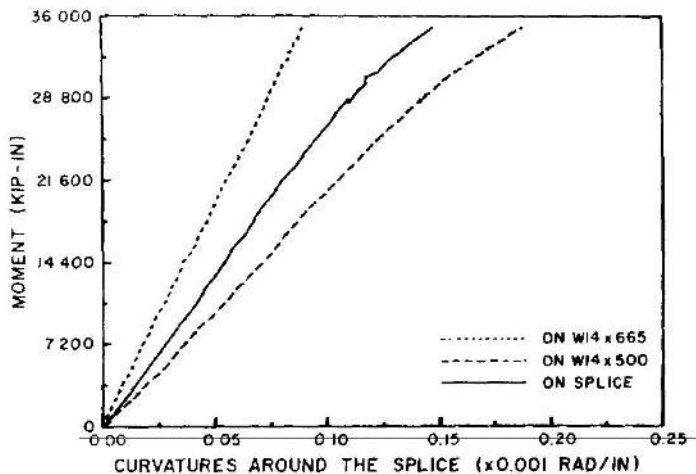

Fig. 15. Moment-curvature from clip gages on partial penetration specimen.

Analysis of Probable Stresses

Attempts to deduct the magnitude of stresses at the critical section using simple traditional design methods can be deceiving. Using assumptions of linear elastic behavior, stresses at failure can be estimated at different cross-sections along the weld as shown on Fig. 16. Calculated maximum stress at the top of the cross sections would be 44.5 ksi at section B-B and 43 ksi at section B'-B'. This is assuming that the effective cross-section at the splice is increasing along a 45-degree angle from the root of the weld. Taking instead an average effective thickness of 2.25 in. on section B'-B' would produce a maximum stress of 51.5 ksi. These calculations indicate that these critical sections would have been elastic or, at worst, slightly starting to yield when failure occurred. The thickening of the section due to the transition welds provides one reason for the apparently higher than expected capacity of the splice. Further, the stresses calculated by these simplified methods would have been a lot higher if the edges of flanges had not been smoothly connected by welding material.

Obviously, these methods neglect the very important effect of stress concentration. Some finite element analyses were conducted to determine the stress's distribution near the splice at the time of failure. In a first approximation, the tension flange was conservatively modeled as a plain strain slice of linear elastic elements continuously supported at the webflange location. Although the presence of discontinuities
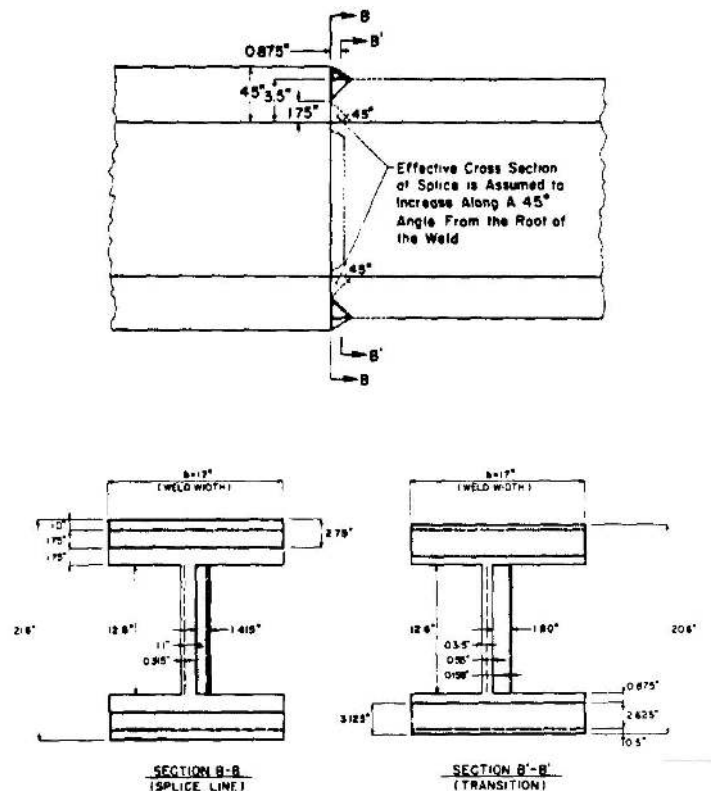

Fig. 16. Definition of various effective cross-sections at the splice for partial penetration specimen.
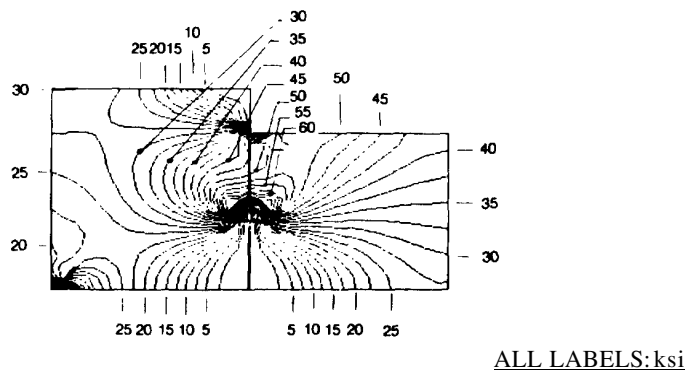
in the mesh to model the unwelded part of the flange makes the results somewhat inexact, the refined analytical procedure qualitatively reveals the stress distribution across the depth of the section near the weld and demonstrates the general behavior of the specimen in the presence of a crack (the unwelded part of the flange).

To estimate the true stresses at the tip of the crack, a very fine mesh would be required in that critical zone, and a more realistic modeling of the boundary conditions would be necessary. A more refined model would also need to consider material non-linearity and fracture. Further, the use of a two-dimensional model does not reflect the variations induced by lateral effects, or shear lag.

Two different models of the flange were investigated and their respective behavior compared. Nodal loads approximating the states of stress in the flanges away from the splice at the time of failure were imposed to each model. In Model 1 (Fig. 17) the two steel sections are welded and left with the change of flange thicknesses unsmoothened. Less experienced welders have been observed leaving welds finished as in Model 1. A mesh of 576 regular elements was generated for this model. The distribution of principal stress σ_1 shown in Fig. 17 indicates a substantial stress concentration at the tip of the crack and at the discontinuous edge joining the two sections. Figure 18 re-emphasizes the fact that while uniformly varying stresses would be expected away from the weld, very high stresses would concentrate at the tip of the crack. Stresses much higher than yield are predicted, thereby violating the assumptions in the analyses.

In Model 2 (Fig. 19), the weld provides a progressive transition to the flange thicknesses, as would be expected in a properly executed weld. In this case, a mesh of 522 elements was used. Smoothening the weld does not change the basic nature of the results but helps to reduce the overall stresses and discontinuity effects, as seen in Fig. 20.

The above finite-element results are useful in revealing the stress concentration effect produced by the unwelded half of the flange and how it acts like a crack. It clearly locates those maximum stresses near the root of the weld and not at the top of the weld, as would be predicted by traditional methods of calculation.

Causes of Failure

Based on the previous observations, the brittle failure observed is apparently the result of a combination of factors. These include excessive stress concentration in the flange due to the crack-like effect of the unwelded part of the flange, bad fusion of the weld passes, critical weld configuration, low effective gage length around the weld, and the size and poor metallurgical properties of the welded sections.

The theoretical capacity of the section has been significantly exceeded. Nevertheless, this failure is rather disconcerting as it occurs in the weld, suddenly, without warning. Moreover, conventional design methods not based on fracture mechanics do not take into account the crack-like discontinuity inherent in partial penetration welds when assessing local stresses.

TEST RESULTS FOR SPECIMEN NO. 2

Description of Testing

Coupons taken from the flange and web of a stub of the W14×370 section used in the full-scale test were machined into standard ASTM tension specimens and tested. The
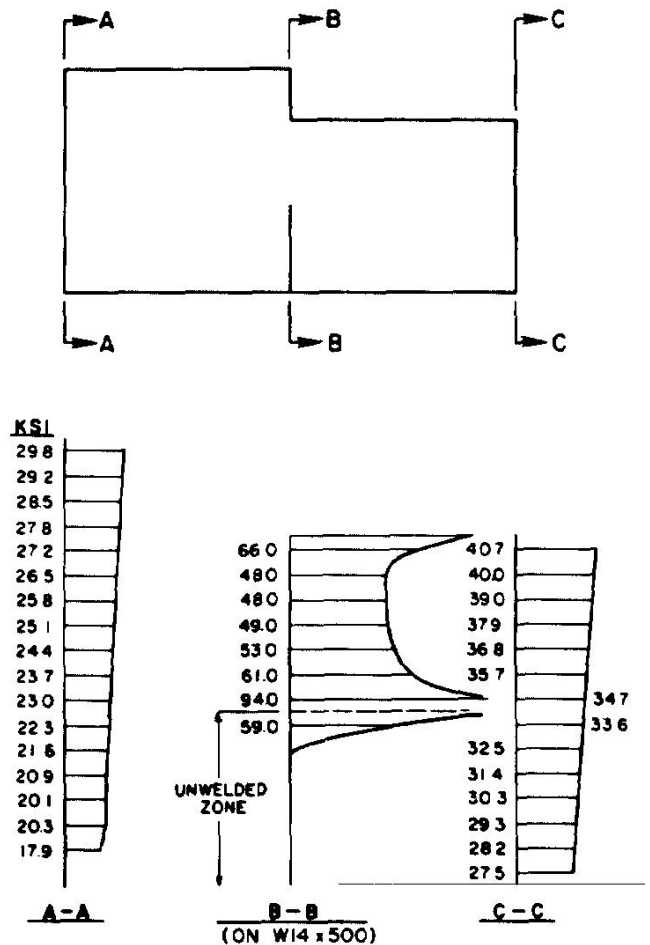
Fig. 18. σ_{11} *stress magnitudes and distribution profile for finite element analysis results along selected cross-sections for Model 1.*

ALL LABELS: ksi

CONTOURS: EVERY 2.5 ksi FROM 0-80 ksi

EVERY 5.0 ksi FROM 80-120 ksi

Fig. 17. σ_{11} *stress contours for finite element analysis of Model 1.*

material taken from the flange and web yielded at 53 and 56 ksi, respectively. Both coupons had a measured elastic modulus E of approximately 29,500 ksi and reached the ultimate strength of 88 ksi. This steel can be considered very ductile, since strains were approximately 0.007 in./in. at the onset of strain hardening, and elongation was around 10% at the initiation of necking.

For the full-scale test specimen, a W14×370 section was connected to a W14×426 section by a full-penetration weld executed as described previously. Since significant yielding could occur in both the smaller section (W14×370) and in the splice area, depending on their relative strengths, two X-Y plots of the moment-curvature relationships for these regions,
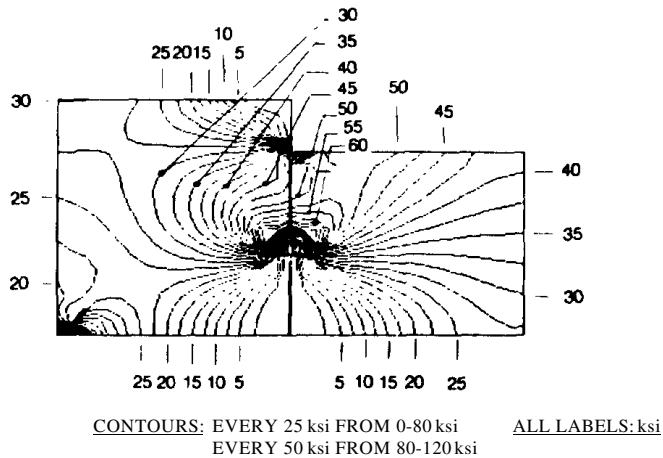

CONTOURS: EVERY 25 ksi FROM 0-80 ksi   ALL LABELS: ksi
EVERY 50 ksi FROM 80-120 ksi

Fig. 19. σ_{11} stress contours for finite element analysis of Model 2.

Fig. 20. σ_{11} stress magnitudes and distribution profile for finite element analysis results along selected cross-sections for Model 2.

as measured by clip-gages pairs, were used to monitor the behavior of the specimen as the loading program progressed. A total of 35 channels of data were recorded for subsequent evaluation. In addition to the types of instrumentation described previously for the Specimen 1, numerous strain gages were installed on the flanges near the splice.

The loading sequence applied is schematically illustrated in Fig. 21. Rather than simply loading the specimen monotonically to a target displacement value as done for Specimen 1, numerous load excursions were employed in each direction before load reversal. By these successive loadings and unloadings to progressively larger force levels, the resiliency and deterioration of the specimen could be measured. In total more than 24 load excursions were applied during one complete cycle of deformation reversal.

As can be seen in Fig. 21, the specimen was first subjected to two load excursions at 60%, 91% and 100% of M_y (the nominal yield moment) of the smaller section, and then loaded in another excursion until an arbitrary small additional plastic curvature was measured. The specimen was coated with a very brittle white paint and, therefore, inelastic regions were easy to identify as yielding produced cracks in the paint. Some yield (Ludder's) lines were locally observed at midwidth on the outer face of the tension flange of the W14×370 near the weld as soon as the ($0.6M_y$) level was reached. More of those lines appeared as yielding progressed. No yield lines were observed on the compression flange in this first stage of the experiment. Large residual stresses were believed to be responsible for this early nonlinearity.

The specimen was then inverted and a similar loading history was applied. Curvatures were used to control the testing process once the nominal M_y level was exceeded. The curvatures obtained in the first part of testing were matched in this part of the test and then exceeded up to an arbitrarily larger value. The nominal value of M_p was also reached at this stage. Yield lines also became apparent during this loading at the web-flange intersection and all through the
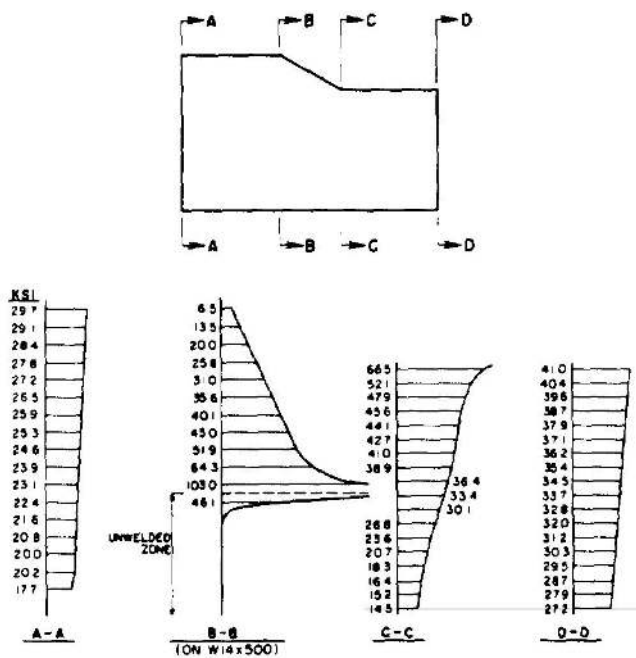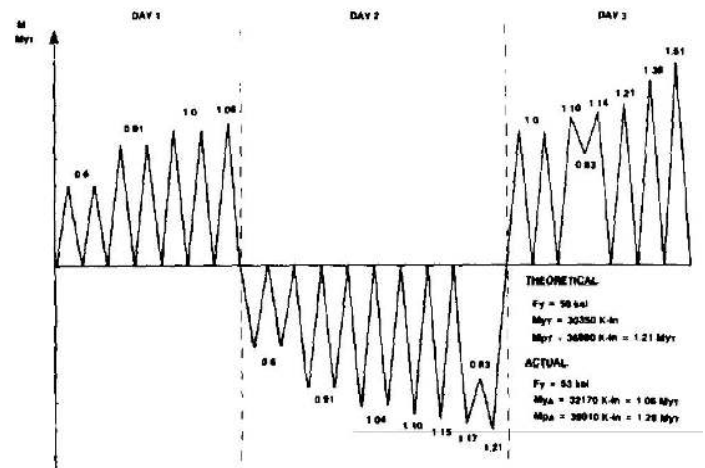

Fig. 21. History of loading applied to the full penetration specimen.

tension flange, and compression yield lines (buckled paint) were visible on the inside of the compression flange.

The specimen was inverted once again in order to complete the displacement cycle. The specimen was loaded directly to yield and then subjected to progressively larger curvature excursions. More yield lines propagated in both flanges and in the web of both sections. In order to simulate interstory drifts that might be anticipated during major earthquakes, the member was loaded until a deflection of 2.4 in. (1.5% of its span) was measured at the splice location. The moment required to reach that state was 25% larger than the nominal value of M_p and 18% more than the actual M_p value (using $F_y = 53$ ksi). Note that M_p is 21% more than M_y for this section. These moments were large enough to induce significant yielding in the W14×426.

In light of the excellent behavior of the specimen, and since the webs of the sections were starting to yield in shear, it was decided not to pursue the loading any further. Large residual deformations (and stresses) remained after unloading. The weld behaved very well and was undamaged.

Analysis of Results

All the various instruments located on the specimen recorded regular, "full" hysteresis loops, and no deterioration in properties from excursion to excursion was noticed.

Moment-curvature relationships as deduced from the clip gages are presented in Fig. 22. The clip-gage set crossing the weld splice measured more yielding during that first part of the experiment than the other sets located on the individual sections. Apparently the W14×370 started to yield first, very close to the weld where the tension residual stresses induced by weld shrinkage were probably the highest (the clip-gage set crossing the weld also spans some of the W14×370 and
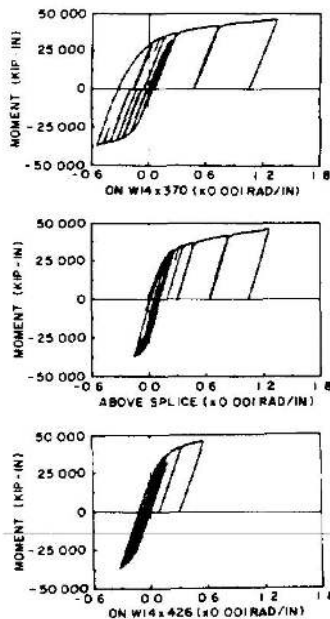
W14×426 sections). Note that significant non-linearity in the splice moment-curvature relation occurs as low as 40% of M_y (nominal). Non-linearity in the moment-curvature relation for the W14×370 also occurs early, at about 60% of M_y (nominal). During the second part of the loading, the clip-gage set above the W14×370 section yielded more than any other. This is due in part to the release of the initial residual stresses as a result of earlier yielding, strain hardening of previously yielded material, and the increased strength and stiffness of the W14×426 also being measured by the central clip-gage set. During the last portion of the load history, it was observed that the W14×370 section yielded the most and that even the W14×426 section was undergoing plastic strains.

Moment-curvature relationships have also been derived from the strain gages located on the web and flanges of the sections (Figs. 23 and 24). Strain gages were installed within ½ in. of each edge of the weld on the outside of the flanges and within $1\frac{3}{8}$ in. on the web. Note that some hysteresis curves are incomplete, as some strain gages failed during testing. These curves are terminated by an "x." In agreement
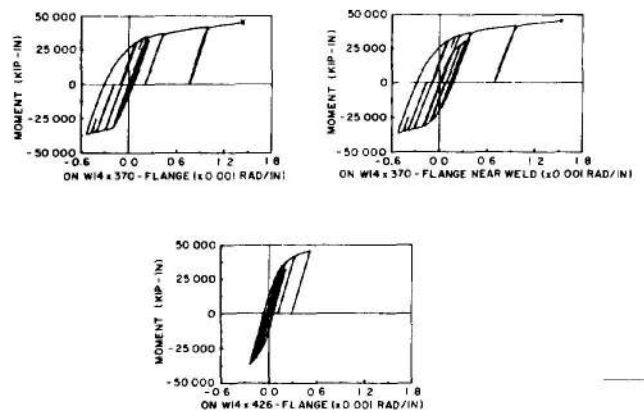

Fig. 23. Moment-curvatures from strain gages on the flange of the full penetration specimen.
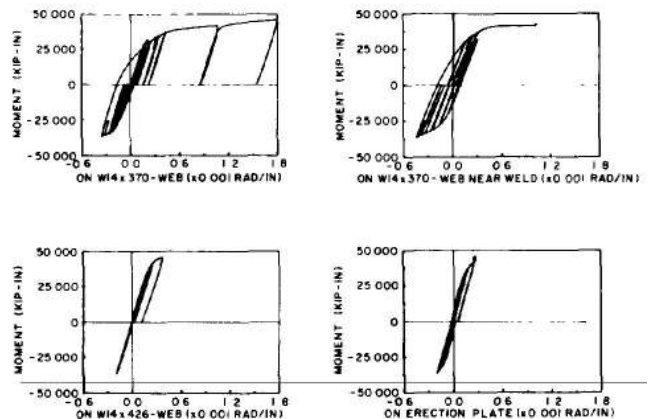

Fig. 22. Moment-curvatures from clip gages on the full penetration specimen.

Fig. 24. Moment-curvatures from strain gages on the web of the full penetration specimen.

	Story	Columns	Beam	Braces
	1	W12×96	W12×106	W12×53
	2	W12×96	W12×106	W12×53
	3*	W12×65	W12×96	W12×53
	4	W12×65	W12×96	W12×53
	5*	W12×40	W12×87	W12×50
	6	W12×40	W12×79	W12×45
	7*	W12×40	W12×45	W12×40
	8	W12×40	W12×45	W12×40

* Splice in column at this level.

	Maximum Forces from UBC Analysis				Allowable Forces		
	Columns		Braces				
Story	Compr.	Tension	Compr.	Tension	Column Compr.	Splice Tension	Brace Compr.
1	−713	426	−186	164	−701	–	−241
2	−582	333	−185	162	−701	–	−241
3	−457	245	−176	154	−472	286	−241
4	−341	166	−162	141	−472	–	−241
5	−236	98	−145	123	−237	177	−146
6	−144	44	−122	101	−237	–	−129
7	−70	7	−95	75	−237	177	−114
8	−15	–	−63	43	−237	–	−63

	Maximum Forces from Nonlinear Analysis				P_y/2 of Smallest Section at Splice
	Columns		Braces		
Story	Compr.	Tension	Compr.	Tension	
1	−1709	1529 Y	−787	784 Y	–
2	−1319	1161	−780	778	–
3	−1068	931 Y	−637	624	478
4	−907	796	−509	494	–
5	−724	635 Y	−429	414	295
6	−522	459	−372	361	–
7	−298	258	−370	357	295
8	−89	73	−253	241	–

Y = Members responded inelastically (yielded).

with what was discussed previously, larger curvatures were recorded close to the weld in the initial phase of loading. This was true even for the W14×426 when the gages on the flanges directly adjacent to the weld were used. In the end, all gages located on the W14×370 section recorded a very large amount of yielding. Irregular bolt sliding and localized yielding around the bolts during the last part of the load history produced the only significant participation of the erection plate in dissipating energy. An irregular spike was recorded by the erection plate strain gages at the end of the testing program when a tack weld connecting the plate to the smaller section failed suddenly.

Ductilities Recorded

Ductility ratio concepts are helpful to quantify the contribution of each section to the energy dissipation of the specimen. The nature of this test justifies using only the most elementary definitions of ductility ratio for this study. The ductility definitions used in Table 2 are presented in Fig. 25. Basically, the measured response quantity is divided by the value obtained at the plastic moment (M_p). Note that this concept of ductility ratio is also based on the nominal steel properties and does not account for residual stresses. Therefore, some judgment must be used in interpreting the results. A ductility ratio of less than 1 does not necessarily mean that behavior is still linear elastic, since residual stresses already induced non-linearity. In any event, since M_p is 21% higher than M_y, non-linear behavior is guaranteed to occur before a ductility ratio of 1 is obtained. A ductility ratio of 1 could have been defined to occur just at the onset

	μ_1^+	μ_2^-	μ_2^*	μ_3^+	μ_3^*
Table 3. Ductilities Measured for Specimen No. 2					
Deflection at center span	1.07	1.39	1.55	3.68	4.02
CLIP GAGES					
W14×370	1.07	2.43	2.62	5.97	7.39
Splice	1.16	0.68	1.18	5.66	5.60
W14×426	0.83	1.44	1.45	2.62	3.13
STRAIN GAGES					
W14×370 web	0.91	1.56	1.74	7.96	8.68
W14×370 web near weld	1.38	1.92	2.36	4.51	5.29
W14×426 web	0.78	0.86	0.91	1.28	1.28
W14×370 flange	1.15	2.36	2.62	6.36	7.71
W14×370 flange near weld	1.68	2.31	3.06	6.79	8.07
W14×426 flange near weld	0.98	1.08	1.36	2.38	2.65
Erection plate	0.31	0.39	0.42	0.56	0.61

of yielding (and resulting ductilities would have been larger than reported here), but it was thought that the definition adopted here was more standard and practical from a design perspective. Measured ductilities as defined in Fig. 25 are tabulated in Table 3. Final curvature ductility ratio on the W14×370 was approximately 6. The curvature ductility ratio developed over the splice region was only slightly smaller. Since the specimen was not tested to failure, ultimate ductilities would evidently be larger.

DISCUSSION OF RESULTS

Partial Penetration Weld

A partial (half) penetration butt weld connecting two of the largest heavy jumbo steel sections available has been tested. The final capacity of the splice exceeded by more than 25% the predicted capacity based on the effective dimensions of
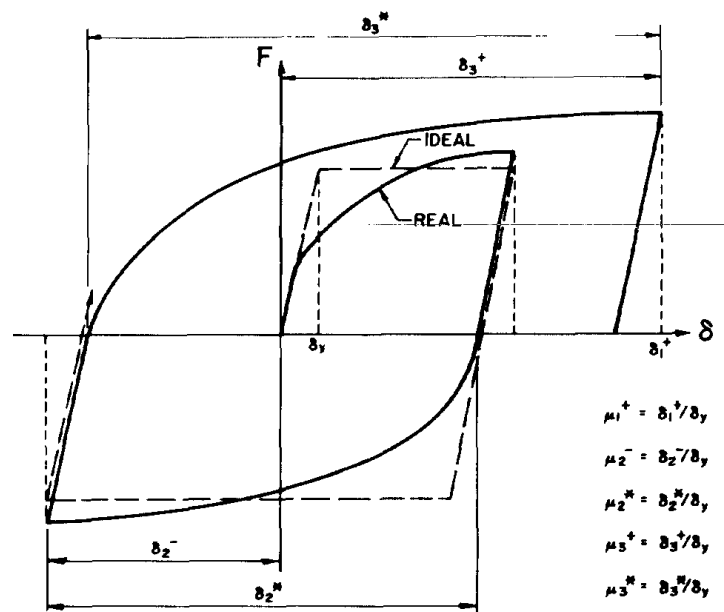

$$\mu_1^+ = \delta_1^+/\delta_y$$
$$\mu_2^- = \delta_2^-/\delta_y$$
$$\mu_2^* = \delta_2^*/\delta_y$$
$$\mu_3^+ = \delta_3^+/\delta_y$$
$$\mu_3^* = \delta_3^*/\delta_y$$

Fig. 25. Ductility definitions used.

the smaller member joined. The smooth transition between the smaller and larger sections at the splice created an enlarged weld surface which may be in part responsible for the increased strength. Nonetheless, simple design calculations are deficient in predicting the state of stress of the critical section. The implications of this for other weld configurations must be carefully assessed.

The splice failed in a very brittle manner when tested under pure bending. Numerous factors, as outlined earlier, contributed to produce the observed brittle behavior. The effect of axial loads on this splice has been analytically simulated in Ref. 7.

It is not known at this stage if all partial penetration butt welds will behave similarly irrespective of the welded specimen thickness or the degree of penetration. This test and previous research on Group 4 and 5 steel sections (as well as simple fracture theory) implies that the risk of brittle failure is increased with large steel thicknesses.

This observed brittle behavior creates a risk of particular interest in seismic regions where it is recognized that codecalculated forces may be largely exceeded by actual earthquake-induced actions. These considerations have been further discussed by the authors elsewhere.[7] Nevertheless, designers should be aware of the potential adverse behavior of this detail and use it in circumstances only where it will not be a structural weak link.

Full Penetration Weld

As cycling progressed on this specimen, the W14 × 370 increased its contribution to the energy dissipation. Although the plasticity started near the welds on the W14 × 370, it progressed quickly along the whole segment of the W14 × 370 under uniform moment, leaving the weld free of excessive straining. This appears to be a very desirable behavior. Nevertheless, non-linearity in the moment-curvature relations was noticed very early during the first part of testing. In some locations, non-linearity occurred at less than half M_y.

Considering the importance of ductility in seismic-resistant design where full penetration welds on such sections are often specified, the excellent ductile behavior experimentally obtained with this type of butt weld, when properly executed, is most significant. Nevertheless, one must recognize that this research program partly originated because full penetration butt welds of ASTM A6 Group 4 and 5 rolled sections have reportedly failed in a brittle manner under very low loads. Although this test has not simulated this previously reported failure mode, it showed instead that a full penetration butt weld on steel rolled sections of large thickness can have satisfactory behavior, provided the engineer and fabricator take the necessary precautions in using a good weld geometry, welding sequence, preheating, interpass temperature, controlled cooling rate, and ultrasonic inspection. It is significant to note that in the specimen tested here, the copes were ground smooth, the root pass for the full penetration weld was

located in the backup bar, the web was welded completely prior to welding the flanges, cooling rate was controlled, and continuous inspection was utilized.

CONCLUSIONS

Partial Penetration Splices

A half penetration butt weld connecting two heavy jumbo steel sections, and tested in pure bending, has been able to develop and exceed its nominal design capacity. However, it failed in a very brittle manner partly as a consequence of a severe stress concentration created by the unwelded part of the flange, as well as due to a series of concurrent metallurgical and welding factors inherent to these type of details when used for heavy steel section splices. Continuous visual inspection during welding and ultrasonic testing of the base metal and welds was not sufficient to avoid this undesirable failure mode.

Where such welds are to be used, care must be taken to ensure that (1) splices would not be expected to yield under realistic loading conditions or (2) a brittle failure of the splice would not impair the stability of the structure.

Full Penetration Splices

A full penetration butt weld connecting two heavy steel sections and tested in pure bending has been able to develop its full strength and exhibit considerable ductility. Although the plasticity started near the weld in the W14×370, it progressed quickly along the whole segment of the W14×370 under uniform moment, leaving the weld free of excessive straining. This is a very desirable behavior.

This test has not simulated the failures case previously reported for several full penetration butt welds of ASTM A6 Group 4 and 5 rolled sections, and therefore the added planning and quality control procedures, as well as the necessary precautions described previously, should be accounted for in reviewing the satisfactory behavior of the test specimen. The implications of these conclusions to other weld configurations should be carefully assessed.

ADDITIONAL RESEARCH NEEDS

Considerable theoretical and metallurgical research needs to be performed to understand the interaction of all the factors contributing to the performance of heavy weldments. This work would lead to reliable analytical techniques for predicting the behavior of welds and would improve our ability to prescribe dependable weld designs and procedures. In particular, improvement of fracture mechanics techniques applicable to the welds in question would be desirable. However, from a practical design point of view, additional research is also needed to assess the global behavior of splices between heavy rolled sections.

Given the brittle nature of the failure observed in the partial penetration splice, it is desirable to quantify scale effects to see if similar brittle failures are observed with smaller sections or with greater penetrations on large sections. In view of the high cost of full penetration splices, it would be desirable to investigate alternative partial penetration details presenting improved ductility while preserving economy. The ability of details, such as double web shear plates (or channels), to reposition a partial penetration weld splice after fracture should also be investigated. While conventional design procedures provide conservative estimates of strength for this case, simple analysis procedures for computing strengths of other configurations are needed.

Finally, this limited study has presented one case of a full penetration butt-weld splice of heavy-rolled steel sections having a satisfactory behavior. In view of the reported failures of similar splices, further studies should be undertaken in order to improve the present understanding of the effect of the various factors identified as having a negative influence on the integrity of this type of detail for heavy steel sections.

For both types of splices the effects of axial load and shear remain to be investigated. In addition, research related to the use of other types of welding procedures (e.g., SMAW and GMAW) should be performed.

REFERENCES

1. American Institute of Steel Construction, Inc., "Commentary on Highly Restrained Welded Connections," *Engineering Journal,* 10(3rd Quarter, 1973).
2. American Institute of Steel Construction, Inc., "Specifications for the Design, Fabrication and Erection of Structural Steel for Buildings with Commentary," in *Manual of Steel Construction,* 8th ed, and "Supplement No. 2," effective January 1, 1989 (Chicago: AISC, 1980)
3. American Welding Society, "Fundamentals of Welding," in *Welding Handbook: Vol. 1,* 7th ed. (Miami: AWS, 1976).
4. Bjorhovde, R., "Welded Splices in Heavy Wide-Flange

Shapes," in *Proceedings of the National Engineering Conference and Conference of Operating Personnel, April 29-May 2, 1987, New Orleans, LA,* (Chicago: AISC, 1987).

5. Blodgett, O. W., *Why Welds Crack—How Cracks Can Be Prevented,* Publication G230, (Cleveland, OH: The Linden Electric Co., April, 1977).

6. Blodgett, O. W., *Distortion ... How to Minimize It with Sound Design Practices and Controlled Welding Procedures Plus Proven Methods for Straightening Distorted Members,* Publication G261, (Cleveland, OH: The Linden Electric Co.).

7. Bruneau, M., Mahin, S. A., Popov, E. P., *Ultimate Behavior of Butt Welded Splices in Heavy Rolled Steel Sections,* EERC Report No. 87-10, (Berkeley: University of California, Earthquake Engineering Research Center, September, 1987).

8. Collins, A., welding consultant, private communication.

9. Doty, W. D., "Procedures for Thermal Cutting and Welding Heavy Structural Shapes," in *Proceedings of the National Engineering Conference and Conference of Operating Personnel, April 29-May 2, 1987, New Orleans, LA,* (Chicago: AISC, 1987):16-1.

10. Fisher, J. W., Pense, A. W., "Experience with Use of Heavy W Shapes in Tension," *Engineering Journal,* 24(2nd Quarter, 1987):63-77.

11. Kaufmann, E. J., Stout, R. D., "The Toughness and Fatigue Strength of Welded Joints with Buried Lamellar Tears," *Supplement to the Welding Journal,* American Welding Society, November, 1983.

12. Mahin, S. A., Bertero, V. V., "Problems in Establishing and Predicting Ductility in Aseismic Design," *International Symposium on Earthquake Structural Engineering, August, 1976, St. Louis, MO,* pp. 613-628.

13. Nippon Steel Corporation, *Welding Manual for Heavy Wide Flange Shapes,* September, 1983.

14. Park, R., Paulay, T., *Reinforced Concrete Structures,* (New York: John Wiley & Sons, 1975).

15. Popov, E. P. and Stephen, R. M., *Tensile Capacity of Partial Penetration Welds,* EERC Report No. 70-3, (Berkeley: University of California, Earthquake Engineering Research Center, October, 1976).

16. Preece, F. R., *Structural Steel in the 80s—Materials, Fastening and Testing,* (San Francisco: Steel Committee of California, 1981).

17. Rolfe, S. T., Barsom, J. M., *Fracture and Fatigue Control in Structures—Application of Fracture Mechanics,* (Englewood Cliffs, NJ: Prentice Hall, 1987).

18. Rooke, D. P., Cartwright, D. J., *Compendium of Stress Intensity Factors,* (London: Her Majesty's Stationery Office, Procurement Executive, Ministry of Defense).

19. Structural Engineers Association of California, Seismology Committee, *Recommended Lateral Force Requirements and Tentative Commentary,* 1988.

20. Tuchman, J. L., "Cracks, Fractures Spur Study," *ENR Magazine,* August 21, 1986.

21. International Conference of Building Officials, *Uniform Building Code,* California, 1988.

22. Yurioka, N., Suzuki, H., Ohshita, S., Saito, S., "Determination of Necessary Preheating Temperature in Steel Welding," *Supplement to the Welding Journal,* American Welding Society, June, 1983.